Research on 3-D Bio-printing Molding Technology of Tissue Engineering Scaffold by Nanocellulose/gelatin Hydrogel Composite

Chen Feng,[a] Ji-ping Zhou,[b] Xiao-dong Xu,[a] Ya-ni Jiang,[b] Hong-can Shi,[c] and Guo-qi Zhao [a,]*

In the biomedicine field, three-dimensional (3-D) printing of biomaterials can construct complex 3-D biological structures such as personalized implants, biodegradable tissue scaffolds, artificial organs, *etc*. Therefore, nanocellulose/gelatin composite hydrogels are often selected as bio-printing materials in the 3-D printing of biological scaffolds. Process parameters of 3-D printed bio-scaffolds were studied in this work because formation accuracy of scaffolds is an important part of the molding process. Firstly, the mixing proportion of nanocellulose and gelatin was explored, and the optimum proportion was selected. Then, the printing effects of different printing pressures, temperatures, speeds, and nozzle diameters were used in the 3-D printing. The filament widths were used to evaluate the molding effects. Finally, through the calculation and analysis of the grey correlation coefficient and grey correlation degree, the multi-objective optimization of the parameters was carried out. The combined effects of the process parameters and the influence degree order on the evaluation index were obtained. Using these parameters, the 3-D porous biological scaffolds were printed with high precision. Furthermore, using a microscope, the morphologies of CCK-8 cells were observed and the cell proliferation were analyzed. The results demonstrated that the printed bio-scaffolds had good biocompatibility.

Keywords: 3-D printing; Biological scaffolds; Technological parameters; Grey relational degree method; Biocompatibility

*Contact information: a: College of Animal Science and Technology, Yangzhou University, Yangzhou 225009, China; b: College of Mechanical Engineering, Yangzhou University, Yangzhou 225127, China; c: College of Medical, Yangzhou University, Yangzhou 225009, China; c: Yangzhou Polytechnic Institute, Yangzhou 225127, China; *Corresponding author: jpzhou@yzu.edu.cn*

INTRODUCTION

It has been a challenge in the scientific and engineering communities to develop a tissue engineering scaffold and organ printing technology based on three-dimensional (3-D) printing (O'Brien *et al*. 2014). In the past few years, the emergence of nanomaterials has provided a new method for improving hydrogels, which requires only a few fillings that could greatly improve the toughness (Liu 2011). Previous studies report on fabricating 3-D scaffolds using a 3-D inkjet printing approach, which utilizes sodium alginate and collagen as raw materials and a calcium chloride solution as both a cross-linking agent and support material (Christensen *et al*. 2015; Hong *et al*. 2015). In addition, a 3-D scaffold was also made by a 3-D printing method using gelatin as the raw material (Lee *et al*. 2014; Bhattacharjee *et al*. 2015; Xiong 2015).

Nanocellulose, as a natural material from grass and other sources of cellulose, has a high strength, aspect ratio, biodegradability, extensive sources, and low cost (Fu *et al*. 2013; Lu *et al*. 2013; Foresti *et al*. 2017). Nanocellulose and its derivatives have been widely used in biomedicine and medical cosmetology (Lu *et al*. 2014; Pietrucha *et al*. 2016; Yoon *et al*. 2016) because it is favorable to release bioactive substances (Mariano *et al*. 2014; Shankar and Rhim 2016; Jiang *et al*. 2017).

Nowadays, CNC and its derivatives have been reported to be used as a viscosifier to improve the viscosity in the process of biological 3D printing (Shao *et al*. 2015). When CNC is added into hydrogel, many hydroxyl groups will be present on the surface of CNC. Thus, there will be strong interaction between CNC molecules, which will enhance the cohesion of hydrogel and increase the apparent viscosity. The increase of viscosity will be beneficial to maintaining the shape of hydrogel scaffold in the process of biological 3D printing (Wei *et al*. 2015).

Generally, the extrusion pressure, speed, temperature, and nozzle size may affect the freeze-casting of composite materials during the molding process of pneumatic condensation extrusion. To solve problems of over-accumulation, lap deficiency, and slobbering during the condensation extrusion, it is necessary to find a series of accurate control parameters that are suitable for a nanocellulose/gelatin composite hydrogel. In the present study, a nanocellulose/gelatin composite hydrogel was used as the bio-printing material to explore the effects of process parameters including printing pressure (Jiang 2018), temperature, speed, and nozzle diameter on the formation accuracy of bio-scaffolds. The results provided insights into the development of other materials and a relevant forming process.

EXPERIMENTAL

Materials

The nanocellulose (CNC) was extracted from the stem of humulus (HJS), a kind of grass taken from the wild (Yangzhou, China) (Jiang *et al*. 2015). Gelatin (GEL) was bought from Aladdin Chemistry Co. Ltd. (Shanghai, China). To test the bio-scaffold compatibility, human fibroblasts were cultured in Dulbecco's modified eagle medium (DMEM). The CCK-8 cell viability assay kit (Shanghai Ruichu Biotech Co., Ltd., Shanghai, China) was used to test the cell proliferation and cell cytotoxicity.

Methods

Experimental equipment for 3-D printing

A platform-assisted 3-D printing system (Regenovo Biotechnology Co. Ltd., Hangzhou, China) was implemented in this study (Fig. 1a). The 3-D printing system used for the gelatin composite hydrogel was mainly equipped with a pneumatic extrusion device, a testing device, a temperature controlling device, a nozzle, and a receiving platform (Fig. 1b).

Experimental equipment for biocompatibility

To test the biocompatibility, equipment including a commingler (Shanghai Ruichu Biotech Co., Ltd., Shanghai, China), a cell culture incubator (Thermo ScientificTM, China) containing 5% CO_2, a high temperature sterilizing oven (Deke Biotechnology, Shanghai, China), a laboratory centrifuge, a high temperature water bath

(Deke Biotechnology, Shanghai, China), a vibrator (Sunshine, Shenzhen, China), and an enzyme-labeling instrument (Thermo ScientificTM, China) was used.

Specimen preparation

Certain amounts of gelatin (GEL) were added to a phosphate buffer solution (PBS) at 40 °C and mixed until completely dissolved. Then, different amounts of CNC suspension with a 1% concentration were added to the GEL solution and stirred for one hour at 40 °C. The mixture was then deaerated in a vacuum. Finally, the GEL concentration in the hydrogels were 5% while the CNC concentrations were 0%, 5%, 10%, and 15%. These concentrations were designated as GEL-5, 5%-CNC/GEL-5, 10%-CNC/GEL-5, and 15%-CNC/GEL-5 (Table 1), respectively.

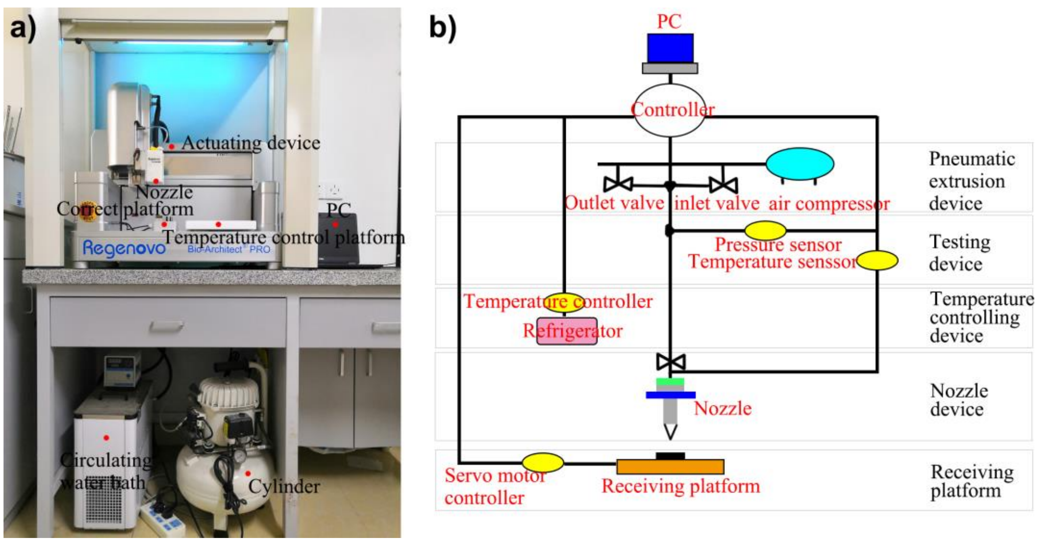

Fig. 1. (a) Photograph of 3-D printer, (b) the establishment of 3-D printing system

Table 1. Chemical Composition of Hydrogel Samples

Samples	GEL Content (%)	GEL Concentration (mg.mL^{-1})	CNC Content (%)	CNC Concentration (mg.mL^{-1})	Total Solids Concentration (mg.mL^{-1})
GEL-5	5	50	0	0	50
5%-CNC/GEL-5	5	50	5	2.5	52.5
10%-CNC/GEL-5	5	50	10	5	55
15%-CNC/GEL-5	5	50	15	7.5	57.5

Three-dimensional printing method

The hydrogel materials were printed using a pneumatic extrusion method. The hydrogel stored in the cartridge entered into the irregular transition flow channel and then into the conical nozzle. It was extruded from the nozzle to form a filament. Secondly, the printer moved the nozzle according to the designed route in the platform and formed the designed pattern in the first layer. Once a layer was completed, the nozzle was raised to a higher height and the process was repeated until the pattern was complete. After printing, the filamentous hydrogel formed a specific 3-D scaffold structure according to the preset trajectory.

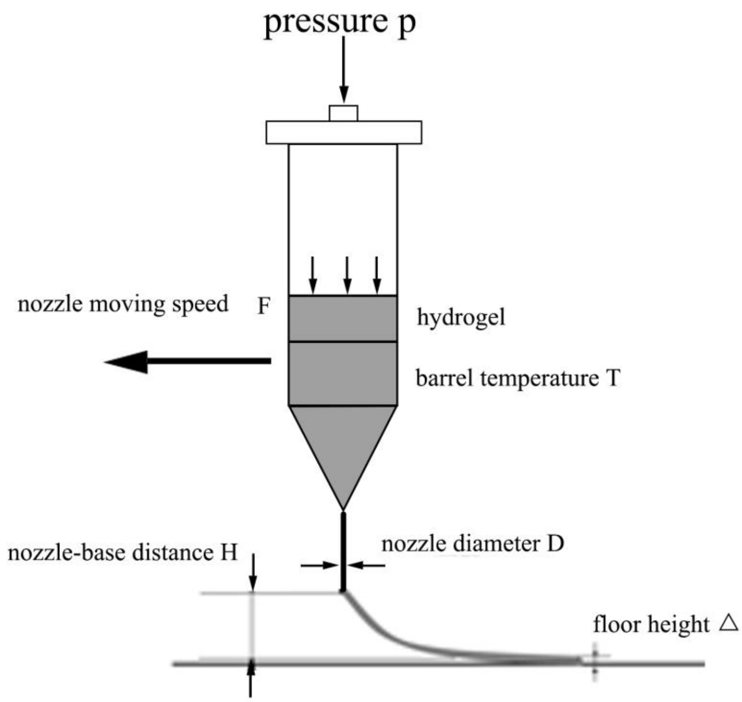

Fig. 2. Graphic of printing parameters in hydrogel printing

Printing setup

The rapid prototyping method of pneumatic condensation extrusion was selected according to the biological composite characteristics in this study. During the molding process, the extrusion pressure, speed, and temperature, as well as the nozzle size may affect the freeze-casting of the composite materials, as shown in Fig. 2. To evaluate the effects of the relevant parameters during the forming process, multiple experiments were designed.

The first experiment evaluated the molding process when the hydrogel concentration was changed and all other printing parameters remained consistent. The samples GEL-5, 5%-CNC/GEL-5, 10%-CNC/GEL-5, and 15%-CNC/GEL-5 were used to print a circle. The extrusion filamentous hydrogel widths and altitudes were measured and recorded at 0 s and 15 s after printing finished.

The second experiment evaluated the molding process when different nozzle diameters were used and all other printing parameters remained consistent. The samples GEL-5, 5%-CNC/GEL-5, 10%-CNC/GEL-5, and 15%-CNC/GEL-5 were printed using nozzle diameters of 0.21 mm, 0.26 mm, and 0.41 mm, respectively. The extrusion filamentous hydrogel widths were photographed and recorded at 3 min after printing finished.

The third experiment tested the molding process with different printing pressures, while all other printing parameters remained consistent. The samples GEL-5, 5%-CNC/GEL-5, 10%-CNC/GEL-5, and 15%-CNC/GEL-5 were printed under the pressures of 0.05 MPa, 0.06 MPa, 0.07 MPa, 0.08 MPa, and 0.09 MPa, respectively. The extrusion filamentous hydrogel widths were photographed and recorded at 3 min after printing finished.

The fourth experiment evaluated the molding process with different cartridge temperatures, while all other printing parameters remained consistent. The samples GEL-5, 5%-CNC/GEL-5, 10%-CNC/GEL-5, and 15%-CNC/GEL-5 were printed at the cartridge temperatures of 5 °C, 15 °C, 20 °C, and 25 °C, respectively. The extrusion filamentous hydrogels, showing the widths, were photographed and recorded at 3 min after printing finished.

The fifth experiment tested the molding process with different nozzle moving speeds while all other printing parameters remained consistent. The samples GEL-5, 5%-CNC/GEL-5, 10%-CNC/GEL-5, and 15%-CNC/GEL-5 were printed when the nozzle moved at the speeds of 10 mm/s, 15 mm/s, 20 mm/s, and 25 mm/s, respectively. The extrusion filamentous hydrogels, showing the widths, were photographed and recorded at 3 min after printing finished.

Grey relation analysis

Grey relational analysis (GRA) is an impact evaluation model to measure the degree of similarity or difference between two sequences based on the grade of relation. The GRA possesses the merit of point set topology and as such, the global comparison between two sets of data is undertaken instead of compared by measuring the distance between the two points. The process is summarized below.

The i^{th} evaluated object can be described in Eq. 1,

$$X_i = \{X_{i1}, X_{i2},\ldots,X_{ip}\} \quad i=1,2,...,n \tag{1}$$

where the number of alternatives is n and each alternative has p criteria.

The first step was to determine the reference sequence. According to the meaning of each criterion, the optimal value of each criterion is selected from *n* alternatives as the reference sequence X_0, as show in Eq. 2,

$$X_0 = \{X_{01}, X_{02}, \ldots X_{0P}\} \tag{2}$$

where the reference sequence X_0 constitutes a relatively ideal optimal sample and is the standard of comprehensive evaluation. For each criterion, the decision maker should assign weightings and a preference index (PI). If a criterion is positive, a better alternative will occur when the criterion value is higher. If it is negative, X_0 will be the minimum value. If it is a moderate scale, X_0 will be the moderate value.

The second step was normalizing, as shown in Eq. 3,

$$Xij' = \frac{Xij}{Xoj} \quad i=1, 2, ...n; j=1, 2,...p \tag{3}$$

where the optimal value of each index is 1 and the optimal reference sequence after normalizing could be calculated in Eq. 4:

$$X_0 = \{1, 1,\ldots,1\} \tag{4}$$

The third step was to compute the distance of the maximum and minimum difference values (Δ_{ij}). Equation 5 calculates the absolute difference between each alternative sequence and the reference sequence,

$$\Delta ij=|Xij-1|, i=1, 2,\ldots, n; j=1, 2, \ldots,P \tag{5}$$

where the maximum difference was designated as Δ (max), and the minimum difference as Δ(min). Equations 6 and 7 are shown below:

$$\Delta\ (\max) = (\Delta_{ij}) \tag{6}$$

$$\Delta\,(\min) = (\Delta_{ij}) \tag{7}$$

The fourth step was to apply the grey relational equation to compute the grey relational coefficient ζ_{oi}, as shown in Eq. 8,

$$\zeta oi = \frac{\Delta(\min) + \rho\Delta(\max)}{\Delta ij + \rho\Delta(\max)} \tag{8}$$

where ρ is the discrimination coefficient, typically between 0 and 1. In this study, ρ was 0.5.

The fifth step was to compute the grey coefficient degree (γ_{oi}). For each evaluated alternative, the mean value of the correlation coefficient between p criteria and the elements corresponding to the reference sequence was calculated. The correlation relationship between each evaluation alternative and the reference sequence was denoted as γ_{oi} as calculated in Eq. 9:

$$\gamma\,oi = \frac{1}{P}\sum_{K=1}^{p} \zeta_i(k) \quad i=1, 2\,,...n \tag{9}$$

If the weights (W) of criteria are different, the grey coefficient degree (γ_{oi}) was computed through Eq. 10,

$$\gamma oi = \frac{1}{P}\sum_{K=1}^{p} Wk * \zeta_i(k)\quad , k=1, 2,...P \tag{10}$$

where W_k is the weight of each criterion, and for decision-making processes, if any alternative had the highest γ_{oi} value, then it was the most important alternative. Thus, the alternative priorities could be ranked in accordance with γ_{oi} values.

Bio-scaffold compatibility test

First, the hydrogel was sterilized with a syringe filter (0.22 μm). Secondly, 50 μL of sterilized hydrogel was placed in each well of a 96-well plate and kept at 37 °C for 4 h. The unreacted materials were then washed 3 times with a PBS (pH 7.4). A 100 μL PBS was added to the control group. Thirdly, 100 μL cell suspensions were added to the 96-well enzyme plate. The human fibroblasts were grown in 89% DMEM supplemented with 10 vol% heat-inactivated fetal bovine serum and 1 wt.% penicillin-streptomycin under standard culture conditions at 37 °C in an incubator containing 5% CO_2. Fourthly, the cells cultured on the scaffolds were observed using an inverted microscope (at 40 times and 100 times, respectively) after 1, 2, 3, and 4 days of culture. Lastly, 10 μL CCK-8 was added to each well every day. The plate was incubated in the incubator for 2 h, and the absorbance at 490 nm was measured by a microplate reader.

RESULTS AND DISCUSSION

Compatibility Test of Bio-scaffold

The hydrogel concentration determines the strength of the gel particles, and the viscosity recovery of the gel particles was the key factor affecting the molding quality of 3-D printing when the hydrogels were extruded from the nozzle. A concentration gradient of hydrogels was completed to investigate the printing effects (Fig. 3). The results showed that samples GEL-5, 5%-CNC/GEL-5, 10%-CNC/GEL-5, and 15%-CNC/GEL-5 could be extruded from the nozzle successfully. Immediately after printing was finished (0 s), the printing filament diameter of the GEL-5 sample was the largest. The diameter notably decreased when CNC was present as a filler, and 10%-CNC/GEL-5 printed the smallest filaments. Moreover, 3-D printing with GEL-5 and 5%-CNC/GEL-5 was easily dragged and molded unsuccessfully. At the moment of 0 s, the width of filaments reflects the swelling rate of hydrogel when extruded from nozzle. At the moment of 0 s, the width of 15%-CNC/GEL-5 was wider than that of 10%- CNC/GEL -5, indicating that the expansion rate of 15%-CNC/GEL-5 was higher. In addition, at the moment of 15 s, the width of 15%- CNC/GEL -5 was also wider than that of 10%- CNC/GEL -5, indicating that the shrinkage rate of 10%- CNC/GEL -5 was also greater. Thus, at the 10%-CNC/GEL-5 concentration, the hydrogels were well formed in support. However, this concentration displayed an inhomogeneous hydrogel form that led to a failed molding.

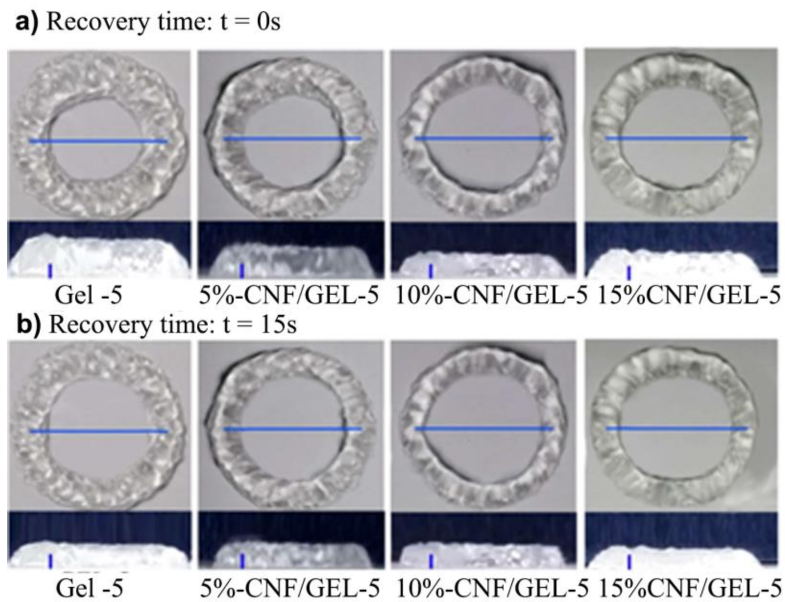

Fig. 3. Printing effects of hydrogel with different concentrations at (a) 0 s and (b) 15 s

Three-dimensional results of 10%-CNC/GEL-5 using nozzles with different diameters

The 10%-CNC/GEL-5 sample was selected to be the most suitable nozzle diameter based on the previous results. As shown in Fig. 4, the nozzle diameter influenced the molding results. During the 3-D printing process, hydrogel flows into the nozzle from the flow channel. Due to sudden changes of the flow channel and the cross-sectional area of the nozzle, fluid pressure is lost. This process is called the damping effect. When hydrogel is extruded, pressure is the power source of hydrogel outflow. Thus, under the same printing pressure, a smaller nozzle diameter caused a greater damping effect and more pressure to be lost (Zhai *et al*. 2010). However, the printing filaments were too thin to mold when the nozzle diameter was too small. Based on these results, the nozzle with a diameter of 0.26 mm was chosen for the following experiments.

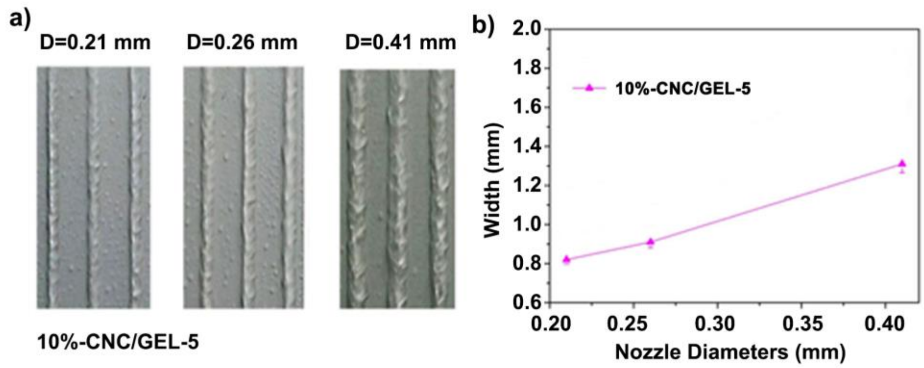

Fig. 4. (a) 3-D printing results of 10%-CNC/GEL-5 using nozzles with different diameters, (b) width changes of printing filaments with time after 3-D printing

Molding results of 10%-CNC/GEL-5 under different printing pressures

In the present study, the pneumatic extrusion molding process was adopted. Therefore, pressure (*P*) was one of the key printing parameters. The pressure should be controlled within a suitable range because if the pressure is too high, a large amount of gels will be extruded, and they will accumulate and collapse on the platform. Furthermore, low pressure will extrude gels slowly and the gels will solidify at room temperature and block the nozzle. In this study, the 10%-CNC/GEL-5 sample was used to print under 0.05, 0.06, 0.07, 0.08, and 0.09 MPa. The extrusion pressure impacted the molding dramatically. Figure 5 shows the variation trend of the printing filament widths with different extrusion pressures. The filament widths increased linearly with pressures, which may have been caused by the pressure changes in the flow channel. A higher pressure resulted in more extruded fluid. In contrast, less pressure caused less extruded flows (Lin-Gibson *et al*. 2003). Thus, the printing filament widths increased with increasing pressures. When the printing pressure was 0.08 MPa, the 10%-CNC/GEL-5 sample had a stable and homogeneous formation. The difference of nozzle inside and outside pressure determines the shape of extrusion filaments. Within the range of the experiment, continuous filaments can be extruded. However, when the pressure was less than 0.05, a large number of breakpoints exist in the filaments. And when the pressure was greater than 0.1, the filaments are too thick to produce excessive accumulation. When the printing pressure was about 0.08 MPa, the 10%-CNC/GEL-5 sample had a stable and homogeneous formation. Thus, the most suitable pressure for the CNC/GEL composite hydrogel was 0.08 MPa.

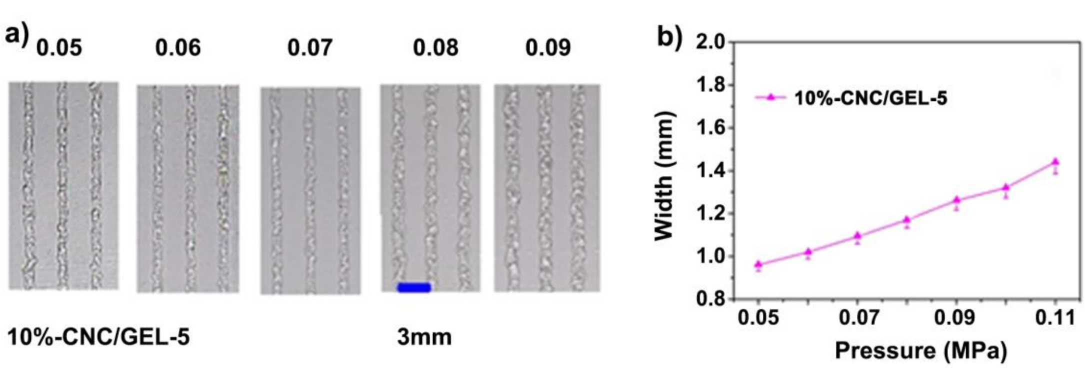

Fig. 5. (a) photos of printing filaments of 10%-CNC/GEL-5 under different printing pressures (b) the change curve of extruded filament widths with printing pressure

Three-dimensional printing results of 10%-CNC/GEL-5 at different temperatures

During the 3-D bio-scaffold fabrication, the material cylinder was heated to ensure the binder viscosity. However, if the temperature was too high, the CNC-gelatin mixture and the original biological compatibility was lost. A temperature within 100 °C did not affect the CNC properties and improved the fluid flow in the channel. Thus, with increasing temperature, the fluid was squeezed out more easily.

As shown in Fig. 6, the filament widths increased linearly with the temperatures. At 5 °C, the filament viscosity was 3.62 Pa•s, while at 15 °C, the viscosity was only 16.31 Pa•s. At 20 °C, the filament widths presented a turning point that over 20 °C, the widths increased precipitously (Fig. 6b). Considering these results, 20 °C was chosen as the most suitable temperature.

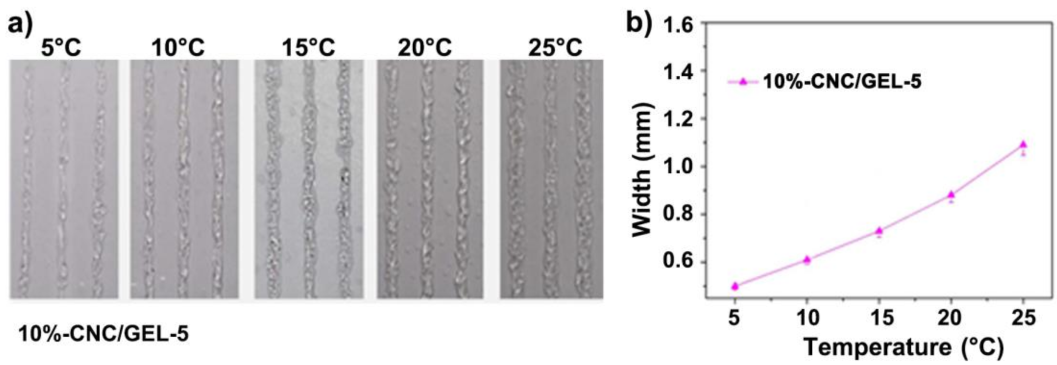

Fig. 6. (a) Photos of printing filaments of 10%-CNC/GEL-5 at different printing temperatures, (b) extrusion filament width variation with printing temperatures

Three-dimensional printing results of different nozzle moving speeds

The printing speed was also one of the most influential factors in the molding process. If the speed is too fast, the forming filament will be too thin and will cause breakpoints easily in the support. In contrast, too low speed will make too much hydrogel diffuse outward, causing the hydrogel to be deposited at an inaccurate position. In the present study, the effects of mold forming at the nozzle speed of 10 mm/s, 15 mm/s, 20 mm/s, and 25 mm/s were studied (Fig. 7).

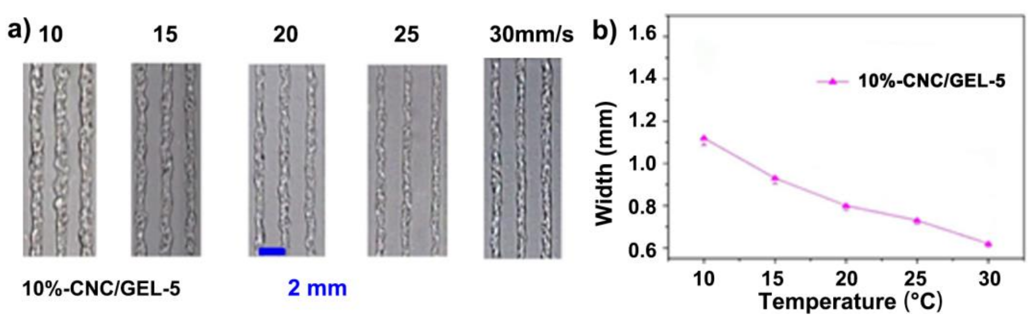

Fig. 7. (a) photos of printing filaments of 10%-CNC/GEL-5 with different nozzle moving speeds and (b) the change curve of extruded filament widths with printing speed

The results showed that the filament widths decreased almost linearly with the nozzle speeds. When the speed was 10 mm/s, the filament width was 1.12 mm (Fig. 7a). A deposition position appeared in front of the nozzle moving site which decreased the printing accuracy. When the speed was 20 mm/s, the filament width decreased to 0.82 mm, and the hydrogel mold was steady, uniform, and accurate. Breaking points appeared when the speed increased to 30 mm/s and the filament width decreased to 0.62 mm. Based on these results, 20 mm/s was selected as the most suitable nozzle moving speed.

Parameter optimization and importance ranking of 3-D printing based on grey relational degree

The 3-D bio-scaffold molding requires good mechanical properties, and the suitable printing parameters are very important. In this research, effects of the molding process were tested and the optimal process parameters were determined. A nozzle diameter of 0.26 mm and filament width were used as the evaluation index of the forming effect. The multi-objective optimization of parameters through the calculation and analysis of the grey correlation coefficient and grey correlation degree was explored (Table 2) (Liu. 2016).

Table 2. 3-D Printing Process Parameters of Original Data

Level (Unit)	Printing Speed A (mm/s)	Printing Temperature B (°C)	Printing Pressure C (MPa)
1	10	5	0.05
2	15	10	0.06
3	20	15	0.07
4	25	20	0.08
5	30	25	0.09

According to the grey relational degree formula, the average relational degree of each factor and its extreme value were calculated. As shown in Table 3, the parameter evaluation was related to the average correlation degree value directly. The parameter was better when the average correlation degree value was higher. Based on these results, the most suitable process parameter combination was obtained as follows: when the nozzle diameter was 0.26 mm, the printing speed was 20 mm/s, the barrel temperature was 15 °C, and the printing pressure was 0.09 MPa. These results were consistent with the experimental results. In addition, the difference between the maximum and minimum value was used to evaluate the impacts of these parameters. Finally, when the printing speed was within 10 to 30 mm/s, the speed was the most important factor to influence the mechanical properties of the 3-D bio-scaffold molding, followed by the printing temperature and pressure.

Table 3. Average Correlation Degree and the Extreme Value of Each Factor

Level	A	B	C
Reference Sequence	1	1	1
1	0.481481482	0.410526316	0.333333333
2	0.65	0.582089553	0.336787565
3	1	1	0.340314136
4	0.65	0.582089553	0.343915344
Extremum	0.518518518	0.417910447	0.01426025

Bio-scaffold compatibility

The cultured cells of the control and treatment groups were observed and photographed (at 40 times and 100 times, respectively) at day 1, 2, 3, and 4 (Fig. 8a). The results showed that there was no considerable difference from day 1 to day 4 under 40x microscopes and the cell densities increased continuously with time. Under 100x microscopes, cells in the control and treatment group were both sparse, spindle-shaped, and presented at the bottom of the 96-well plate on the first day. At this time, the cell densities of the two groups showed no notable differences. Afterwards, from day 2 to day 4, the cell densities increased with time. On the fourth day, cells were arranged closely and the intercellular space was small. In addition, there was no notable difference between the control and treatment group. Throughout the experiment, the cells did not have any pollution and grew well.

The cck-8 reagent was used to test cytotoxicity every day, and the optical density (OD) value was detected. To test the significant differences of cell numbers between the control and treatment group, the Student's t-test at the probability level of 0.05 ($p < 0.05$) was used. The data analysis was performed by Graphpad 20 (Harvey Motulsky, San Diego, CA, USA). As shown in Fig. 8b, there was no significant difference in the number of cells between the experimental group and the control group. Taken together, hydrogels had no toxic effect on the cells.

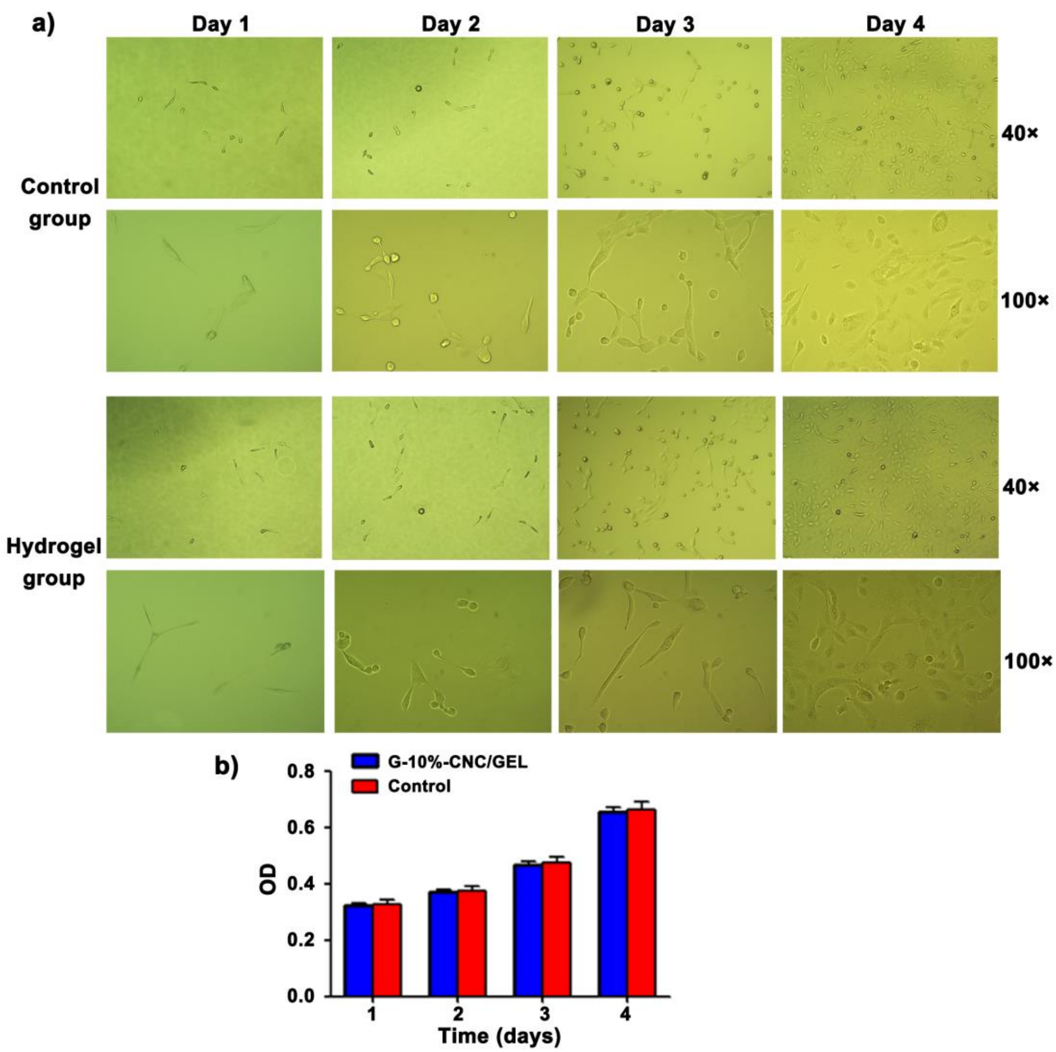

Fig. 8. (a) Microscope images of fibroblasts cultured on medium with hydrogel and without-hydrogel (b) the cytotoxicity testing results

CONCLUSIONS

1. Using the optimal strategy, the printed filaments were well-distributed, and the porosity was clear and without cytotoxicity.
2. The nanocellulose concentration and the printing parameters were the two major impact factors during the 3-D printing bio-scaffold using a nanocellulose/gelatin composite hydrogel. Under a 0.26 mm nozzle diameter with a barrel temperature of 20 °C, a printing pressure of 0.08 MPa, and a speed of 20 mm/s, the suitable width and well molding filaments could be 3-D printed.
3. The printed scaffolds using 10% - CNC/GEL -5 had the highest elastic modulus and showed the best strength as well as anti-deformation ability.
4. Finally, through the calculation and analysis of grey correlation coefficient and grey correlation degree, the order of influence degree on evaluation index was: printing speed > printing temperature > printing pressure.

ACKNOWLEDGMENTS

This work was supported financially by the National Natural Science Foundation of China (No. 81770018) and Yangzhou - Yangzhou University Science and Technology Cooperation Project (No. SCX2017020015).

REFERENCES CITED

Bhattacharjee, T., Zehnder, S. M., Rowe, K. G., Jain, S., Nixon, R. M., and Saw, W. G. (2015). "Writing in the granular gel medium," *Sci. Adv.* 1(8). DOI: 10.1126/sciadv.1500655

Christensen, K., Xu, C., Chai, W., Zhang, Z., Fu, J., and Huang, Y. (2015). "Freeform inkjet printing of cellular structures with bifurcations," *Biotechnol. Bioeng.* 112(5), 1047-1055. DOI: 10.1002/bit.25501

Fu, T., Wei, X. Y., Li, J. H., and Wang, F. (2013). "Development of natural nano-cellulose from tropical agricultural products," *J. Cellu. Sci. Techo.* 21, 78-85.

Foresti, M. L., Vázquez, A., and Boury, B. (2017). "Applications of bacterial cellulose as precursor of carbon and composites with metal oxide, metal sulfide and metal nanoparticles: A review of recent advances," *Carbohyd. Polym.* 157, 447-467. DOI: 10.1016/j.carbpol.2016.09.008

Hong, S., Sycks, D., Chan, H. F., Liu, F. C., Lin, S., Lopez, G. P., Guilak, F., Leong, K. W., and Zhao, X. H. (2015). "3D printing of highly stretchable and tough hydrogels into complex, cellularized structures," *Adv. Mater.* 27(27), 4035-4040. DOI: 10.1002/adma.201501099

Jiang, Y., Zhou, J., Zhang, Q., Zhao, G., Heng, L., Chen, D., and Liu, D. (2017). "Preparation of cellulose nanocrystals from *Humulus japonicus* stem and the influence of high temperature pretreatment," *Carbohyd. Polym.* 164, 284-293. DOI: 10.1016/j.carbpol.2017.02.021

Jiang, Y. (2018). *Preparation of Grass-Derived Nanocellulose and Gelatin Composite* *and Study on the Forming Mechanism of Bio-3D Printing Skin Scaffold*, Ph.D. Dissertation, Yangzhou University, Yangzhou, China.

Lee, V. K., Kim, D. Y., Ngo, H., Lee, Y., Seo, L., Yoo, S. S., Yoo, P. S., Vincent, P. A., and Dai, G. (2014). "Creating perfused functional vascular channels using 3D bio-printing technology," *Biomaterials* 35(28), 8092-8102. DOI: 10.1016/j.biomaterials.2014.05.083

Lin-Gibson, S., Schmidt G., Kim H., Han, C. C., and Hobbie, E. K. (2003). "Shear-induced mesostructure in nanoplatelet-polymer networks," *J. Chem. Phys.* 119(15), 8080-8083. DOI: 10.1063/1.1609972

Liu, Y. (2011). *Synthesis and Characterization on Gelatin-based Nanomaterials*, Ph.D. Dissertation, Nanjing University of Science and Technology, Nanjing, China.

Liu, S. F. (2016). *Grey Systems: Theory and Application*, Emerald Publishing Limited, China. DOI: 10.1108/GS-08-2016-0024

Lu, Q., Tang, L. R., Lin, W., Huang, B. Chen, X. R., Ou, W., Lin, Z. X., and Lin, D. M. (2013). "Preparation and characterization of nanocrystalline cellulose from *Pennisetum sinese*," *Pratacultural Science* 30(2), 301-305 (in Chinese).

Lu, T., Li, Q., Chen, W., and Yu, H. (2014). "Composite aerogels based on dialdehyde nanocellulose and collagen for potential applications as wound dressing and tissue engineering scaffold," *Compos. Sci. Techno.* 94, 132-138. DOI: 10.1016/j.compscitech.2014.01.020

Mariano, M., El Kissi, N., and Dufresne, A. (2014). "Cellulose nanocrystals and related nanocomposites: Review of some properties and challenges," *J. Polym. Sci. Pol. Phys.* 52(12), 791-806. DOI: 10.1002/polb.23490

O'Brien, C. M., Holmes, B., Faucett, S., and Zhang L. G. (2014). "Three-dimensional printing of nanomaterial scaffolds for complex tissue regeneration," *Tissue Eng. Pt. B-Rev.* 21(1), 103-114. DOI: 10.1089/ten.TEB.2014.0168

Pietrucha, K., Marzec, E., and Kudzin, M. (2016). "Pore structure and dielectric behaviour of the 3D collagen-DAC scaffolds designed for nerve tissue repair," *Int. J. Biol. Macromol.* 92, 1298-1306. DOI: 10.1016/j.ijbiomac.2016.08.029

Shankar, S., and Rhim, J. W. (2016). "Preparation of nanocellulose from micro-crystalline cellulose: The effect on the performance and properties of agar-based composite films," *Carbohyd. Polym.* 135, 18-26. DOI: 10.1016/j.carbpol.2015.08.082

Shao, Y., Chaussy, D., Grosseau, P., and Beneventi, D. (2015). "Use of microfibrillated cellulose/lignosulfonate blends as carbon precursors: Impact of hydrogel rheology on 3D printing," *Ind. Eng. Chem. Res.* 54(43), article no. 151007122517002. DOI: 10.1021/acs.iecr.5b02763

Wei, J., Wang, J., Su, S., Wang, A., Qiu, J., Zhang, Z., Christopher, G., Ning, F., and Cong, W. (2015). "3D printing of an extremely tough hydrogel," *RSC Adv*. 5(99), 81324- 81329. DOI: 10.1039/C5RA16362E

Xiong, S. (2015). *Degradation of Silk Fibroin and the Application of 3D-Printed Bio-Inducible Scaffold in Skin Tissue Engineering*, Ph.D. Dissertation, Zhejiang University, Zhejiang, China.

Yoon, H., Lee, J. S., Yim, H., Kim, G., and Chun, W. (2016). "Development of cell-laden 3D scaffolds for efficient engineered skin substitutes by collagen gelation," *RSC Adv.* 6(26), 21439-21447. DOI: 10.1039/C5RA19532B

Zhai, W., Zhen, X. F., Fu, J. B., Jiang, H. Y., and Liang, Y. C. (2010). "Experimental research on tribiological characteristics of the metal-rubber acetabular socket impregnated PVA-H laye," *Lubr. Eng.* 2010(8).

Article submitted: June 29, 2019; Peer review completed: September 2, 2019; Revised version received: September 18, 2019; Accepted: September 19, 2019; Published: October 4, 2019.
DOI: 10.15376/biores.14.4.9244-9257